

## 論文の内容の要旨

### High-resolution photoelectron spectroscopy studies of ultrathin Si gate oxides

(高分解能光電子分光法を用いた極薄 Si gate 酸化膜に関する研究)

氏名 吳 鎮 浩

#### I INTRODUCTION.

The current ultra large scale integration (ULSI) device technology demands the reduction of the gate-oxide film thickness down to about 1 nm. Therefore the chemical abruptness of the SiO<sub>2</sub>/Si interface which largely affects the performance of MOS devices, and the control of oxide formation on an atomic scale are great importance. However, an atomic-scale understanding of the interface structure and the initial oxidation features is still lacking, since it is difficult to analyze the interface structures with various oxidation states of Si, i.e., Si<sup>1+</sup>(Si<sub>2</sub>O), Si<sup>2+</sup>(SiO), Si<sup>3+</sup>(Si<sub>2</sub>O<sub>3</sub>) and Si<sup>4+</sup>(SiO<sub>2</sub>) components<sup>(1)</sup>.

Although the incorporation of N atoms at the Si-SiO<sub>2</sub> interface proved to be very promising to high-quality ultrathin gate dielectric for Si-based ULSI for low leak current and impurity diffusion barrier, the detailed incorporated N atoms has not been elucidated yet.

In this study, we have investigated (i) the structure and the chemical abruptness of the SiO<sub>2</sub>/Si(001) interface, (ii) the initial oxidation process, (iii) the presence of the metastable oxygen adsorbed on a Si(111)-(7 × 7) surface, and (iv) the structure of nitrated Si-SiO<sub>2</sub> interfaces by high-resolution photoemission spectroscopy.

#### II EXPERIMENTAL DETAILS.

##### II -1 High-resolution angle resolved photoemission spectroscopy (ARPES) beam-line BL-1C @ KEK-PF

A grazing incidence varied line spacing plane grating monochromator (VLS-PGM) has been designed and installed at the Photon Factory bending magnet beamline, BL-1C. The monochromator is designed to satisfy both high resolving power and high photon flux for a high-resolution angle-resolved photoemission study. The resolving power of the beam-line exceeds 10,000 at all the covered energy range of the monochromator with photon flux over 10<sup>9</sup> photons/sec. This beam line is equipped with an angle-resolved photoemission spectroscopy system with a hemispherical electron analyzer mounted on a double axes goniometer (see Fig. 1). The total energy resolution of 70meV at the 140eV of photon energy is achieved for Si

2p from clean Si(111)-7×7 surface.

## II-2 Sample preparation & Measurements

The ultra-thin SiO<sub>2</sub> films were grown by exposing clean Si(100)-2×1 and Si(111)-7×7 substrates held at various temperatures to highly-pure O<sub>2</sub> gas at a pressure of 5×10<sup>-8</sup> torr with changing the oxidation time (2L ~150L : in total). The total-energy resolution was set to ~70 meV at photon energies of 130, 140 eV and the angular resolution to ±2° for all measurements. The angle-resolved Si 2p photoemission spectra were measured by changing the polar emission angle ( $\theta$ ) from 0° to 70°.

In the case of the Si oxinitride, we have measured the Si 2p and N 1s for the various samples; (i) SiN grown by jet vapor deposition (JVD) method, (ii) SiO<sub>x</sub>N<sub>y</sub> grown by rapid thermal nitridation(RTN) method using NO and N<sub>2</sub>O gas and (iii) SiO<sub>x</sub>N<sub>y</sub> grown by exposing 1000 L, 3000L of NO gas.

## III RESULTS and DISCUSSION.

### III-1 Chemical structure of ultrathin SiO<sub>2</sub>/Si(100) interfaces ; high temperature oxidation

We measured the Si 2p core-level shifts of the various oxidation states (Si<sup>1+</sup>, Si<sup>2+</sup>, Si<sup>3+</sup> and Si<sup>4+</sup>) for ultrathin SiO<sub>2</sub>/Si(100) interfaces using high-resolution angle-resolved photoemission and have investigated the depth distribution of the individual oxidation states by measuring the intensities of the different Si 2p components as a function of the polar emission angle. From these results, we constructed a non-abrupt SiO<sub>2</sub>/Si(100) interface model. Figure 2 shows high-resolution angle resolved Si 2p spectrum of SiO<sub>2</sub>/Si(100)

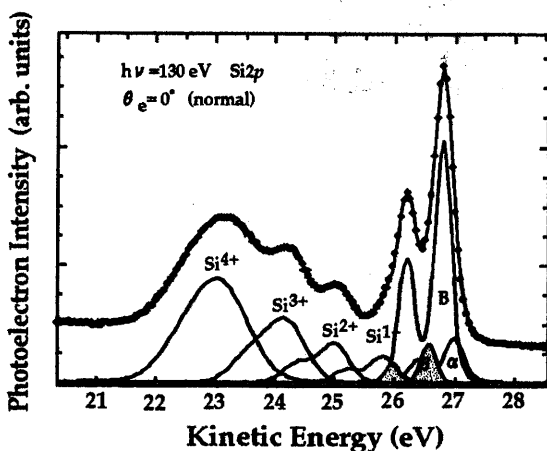


Figure 2 Si 2p spectrum taken from ultrathin SiO<sub>2</sub>/Si(100) at  $\theta = 0^\circ$  with photon energy of 130 eV

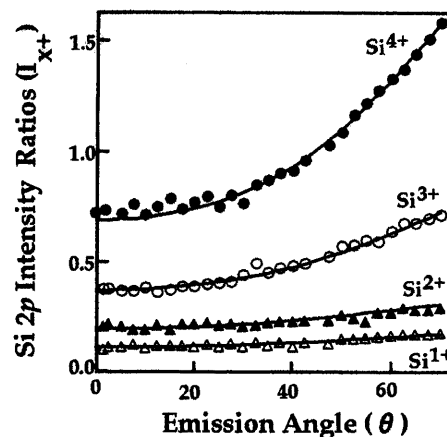


Figure 3 Si 2p intensity ratios of the Si<sup>1+</sup>-Si<sup>4+</sup> components/Si substrate-related components as a function of the emission angle

(150L at 600°C) taken at  $\theta = 0^\circ$ . The spectrum was fitted by a standard curve fitting procedure using Voigt functions with the spin-orbit splitting of 0.60 eV for quantitative analyses. The core-level binding-energy shifts were determined accurately to be 1.00, 1.82, 2.62, and 3.67 eV for Si<sup>1+</sup>-Si<sup>4+</sup>, respectively.

Figure 3 shows the  $\theta$  dependence of the intensities of the individual oxidation states ( $I_{x+}$ ) normalized by the total intensities of the substrate-related components  $I_{Si} = I_B + I_a + I_b$ . The trend of the different  $\theta$ -dependence of Si<sup>1+</sup>/Si<sup>2+</sup> and Si<sup>3+</sup> suggests (i) that the Si<sup>1+</sup> and Si<sup>2+</sup> species have the same depth distribution, most probably at the first interfacial layer and (ii) that the Si<sup>3+</sup> species are distributed in a wider region. The Si 2p intensity variation of each oxidation component ( $I_{x+}$ ) then can be calculated using a simple electron damping scheme<sup>(2)</sup>. The solid lines shown in Fig. 3 are obtained by

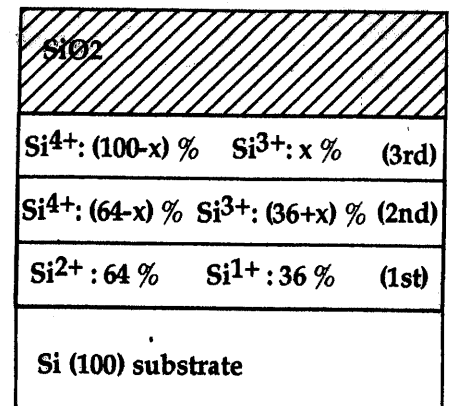


Figure 4 Schematic illustration of the chemical composition of the transition layers based on a chemical non-abrupt model

fitting the experimental data. The optimized transition layers are, 36 %  $\text{Si}^{1+}$  and 64 %  $\text{Si}^{2+}$ , 71 %  $\text{Si}^{3+}$  and 29 %  $\text{Si}^{4+}$ , and 35 %  $\text{Si}^{3+}$  and 65 %  $\text{Si}^{4+}$ , at the first, second and third interfacial layers from the Si substrate, respectively(see Fig. 4). This result thus indicates clearly a chemically non-abrupt interface consisting of three transition layers, which is in contrast to the abrupt interface model <sup>(3)</sup>.

### III -2 Initial oxidation features of Si (100) at room temperature

We have measured the intensities of the different Si 2p components ( $\text{Si}^{1+}$ ,  $\text{Si}^{2+}$ ,  $\text{Si}^{3+}$  and  $\text{Si}^{4+}$ ) as a function of the oxidation time, and discussed the initial oxidation process using a two-dimensional island model based on the experimental results. Figure 5 shows high-resolution Si 2p spectra for (a) 2 L, (b) 12 L and (c) 22 L. The spectra have been decomposed with seven components, one bulk (B), two surface components of Si substrate ( $\alpha$ ,  $\beta$ ) and three sub-oxide components ( $\text{Si}^{1+}$ ,  $\text{Si}^{2+}$  and  $\text{Si}^{3+}$ ) and  $\text{Si}^{4+}$  <sup>(4)</sup>. For the thermal oxidation of Si(100), the intensities of oxidation states are in the order of  $\text{Si}^{4+} > \text{Si}^{3+} > \text{Si}^{2+} > \text{Si}^{1+}$  (see Fig. 2). However, for initial oxidation of Si(100), the intensity of  $\text{Si}^{2+}$  species is the largest. The differences of intensity distribution between thermal oxidation and room temperature (RT) initial oxidation of Si(100) suggest that the concentration of suboxide components during initial oxidation is significantly different from that for typical thermal oxidation process. Figure 6 shows the intensity ratios as a function of the oxidation time.

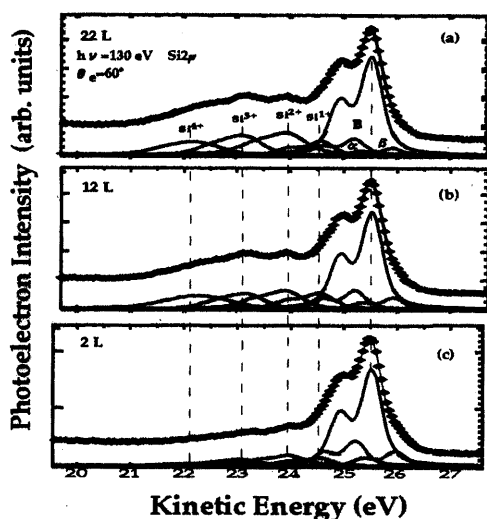


Figure 5 Si 2p spectra taken from 2L, 12L and 22L  $\text{SiO}_2/\text{Si}(100)$  at  $\theta = 60^\circ$  with photon energy of 130 eV.

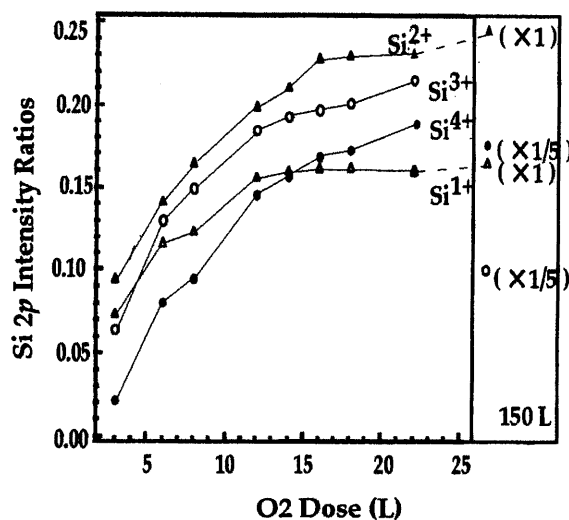


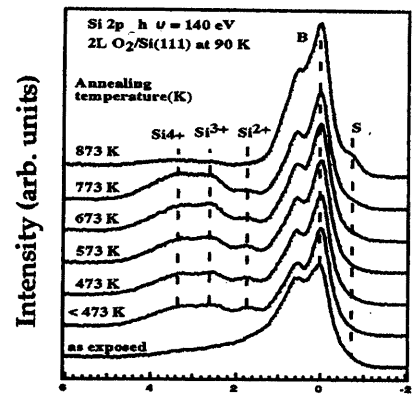
Figure 6 Si 2p intensity ratios of the  $\text{Si}^{1+}$ - $\text{Si}^{4+}$  components/Si substrate-related components as a function of  $\text{O}_2$  exposure

An important result to explain the initial oxidation process is the saturation of  $\text{Si}^{1+}$  and  $\text{Si}^{2+}$  intensities and the continuous increase of  $\text{Si}^{3+}$  and  $\text{Si}^{4+}$  intensities with increasing the oxidation time. In the case of  $\text{Si}^{3+}$  and  $\text{Si}^{4+}$  species, it is possible to assume that the area of the islands containing  $\text{Si}^{3+}$  and  $\text{Si}^{4+}$  are expanding horizontally on the initial oxide layer. We interpret this result as a sign of the initial oxidation caused by the two-dimensional island nucleation.

### III -3 Low-temperature oxygen adsorption on the Si(111)-(7 x 7) surface; oxidation at 90 K

High-resolution photoemission has been applied to the oxygen adsorption on the Si(111)-(7x7) surface at 90 K. We have measured the change of Si 2p binding energy and the intensities of the different Si 2p components ( $\text{Si}^{1+}$ ,  $\text{Si}^{2+}$ ,  $\text{Si}^{3+}$  and  $\text{Si}^{4+}$ ) as a function of annealing temperature. From these results we have revealed the presence of metastable molecular species on the Si(111) surface.

Figure 7 shows the Si 2p spectra for the Si(111) surface dosed with 2L O<sub>2</sub> gas at 90 K and subsequently annealed up to 973 K. After annealing the sample was cooled down to 90 K for high resolution Si 2p measurements. It is observed that the increase of high oxidation species is induced by annealing. The increase (decrease) of Si<sup>4+</sup> (Si<sup>3+</sup>) species induced by annealing means that the configuration changes from the low oxidation state to the high oxidation state. Furthermore, the increase of the high oxidation state indicates that the numbers of O atoms bonded with Si atoms have been increased by annealing, i.e., O atoms should be supplied from the other sites. The dissociation of adsorbed O<sub>2</sub> molecules can supply non-bonding O atoms. Therefore it is possible that the metastable molecular state exist on the Si(111) surface.

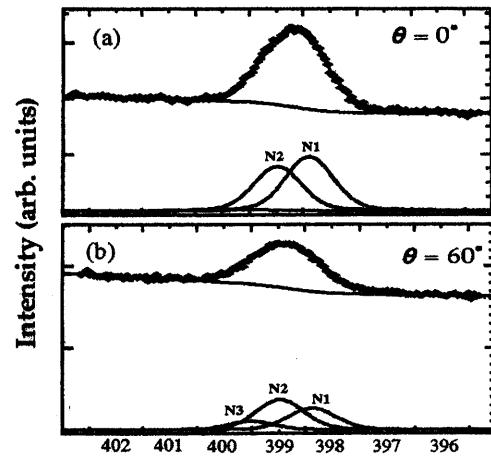


Relative Binding Energy (eV)

Figure 7 High-resolution Si 2p spectra taken for Si(111) exposed to 2L of O<sub>2</sub> at 90 K and subsequently annealed

### III-4 The ultrathin oxynitride/Si(100) interface : Relation between N1s core-level shift and structure

We have measured high-resolution N 1s spectra to investigate the structures of Si-N-O bonding at the nitrated Si-SiO<sub>2</sub> interfaces, and clearly decomposed the N1s peak with two components corresponding to Si<sub>3</sub>N<sub>4</sub> state based on the core-hole relaxation and second neighbor effects<sup>(5)</sup> for the first time. Figure 8 shows N1s spectra of the RTN(using NO gas) sample taken at  $\theta = 0^\circ$  (a) and  $\theta = 60^\circ$  (b). The N1s spectrum has been decomposed with N1, N2 and N3, respectively. Taking into account above mentioned effects, we assigned N1, N2 and N3 as N bonded to three nonoxidized Si atoms, N bonded to fully oxidized Si atoms N[Si(O—)<sub>3</sub>]<sub>3</sub>, and N bonded to two Si atoms and one O atom. Thus, it is suggested (i) that two kinds of Si<sub>3</sub>N<sub>4</sub> species exist at the double interfacial layers and (ii) that the NSi<sub>2</sub>O species are distributed in the region which is more close to the surface.



Relative Binding Energy (eV)

Figure 8 N 1s spectra taken from RTN (NO gas) at emission angle  $\theta = 0^\circ$  (a) and  $\theta = 60^\circ$  (b) with the a photon energy of 500 eV

### IV CONCLUSIONS.

From the results of high-resolution photoemission spectroscopy, we constructed a non-abrupt SiO<sub>2</sub>/Si(100) interface model for thermal oxidation. For initial oxidation on Si(100), the oxidation process at R.T could be explained based on the two-dimensional island nucleation model. We also found the possibility of the presence of metastable molecular species on the Si(111) surface at low temperature. In the case of Si oxynitride, we succeeded in decomposing the N1s peak into two components corresponding to Si<sub>3</sub>N<sub>4</sub> state based on the core-hole relaxation and second neighbor effects. In the near future, for Si oxynitride, we will investigate the annealing dependence of each Si-O-N bonding configurations and the difference of structure between RTN (NO gas) and RTN (N<sub>2</sub>O gas) sample using high resolution photoemission spectroscopy.

### REFERENCES.

1. F. J. Himpsel et al., Phys. Rev. B 38, 6084 (1988).
2. D. A. Luth et al., Phys. Rev. Lett 79, 3014 (1997).
3. M. T. Sieger et al., Phys. Rev. Lett 77, 2758 (1996)
4. H. W. Yeom et al., Phys. Rev. B 59, R 10 413 (1999).
5. G. -M. Rignanesse et al., Phys. Rev. Lett 79, 5174 (1997).